

# Fault Diagnosis of Rolling Bearings Based on SURF algorithm

Hongfang Yuan<sup>1</sup>, Wen Feng<sup>1</sup>, HongWei Qu<sup>2</sup>, Huaqing Wang<sup>2\*</sup>

<sup>1</sup>College of Information Science & Technology

<sup>2</sup>School of Mechanical & Electrical Engineering

Beijing University of Chemical Technology

Beijing 100029

CHINA

yuanhf@mail.buct.edu.cn, fw1989ok@sina.com, quhongwei@outlook.com,

\*Corresponding author, E-mail: hqwang@mail.buct.edu.cn

*Abstract:* - This paper proposed a new method for fault diagnosis of rolling bearings based on SURF (Speeded-Up Robust Features) algorithm, where two-dimension signal is used. Different from other classical 1-d signal processed methods, the proposed method transforms the 1-dimensional vibration signals into images, then image processed methods are utilized to analyze the image signal so as to reach the goal of faulty classification. Images transformed from vibration signals often have special texture features and each faulty category's texture varies. SURF is a computer vision algorithm improved from SIFT (Scale Invariant Feature Transform) algorithm, and it can more efficiently extract local features through the texture of the image. Firstly, normalized time domain vibration signals were converted into gray-scale images. Then the mean filter was employed to complete the image pre-processing. Secondly, local features were extracted from the images by using SURF algorithm. Through the mean-shift clustering algorithm, extracted features were clustered to form a texture dictionary. Finally, features extracted from testing signals were compared with the texture dictionary to determine the corresponding faulty category. To validate the proposed method, several comparative experiments between SURF and SIFT-based algorithm have been carried out. The experimental results indicate that the proposed method outperforms the existing SIFT descriptor in terms of classification accuracy and computation cost for bearing fault diagnosis.

*Key-Words:* - fault diagnosis, rolling bearing, SURF, feature vector, mean-shift clustering, computation cost

## 1 Introduction

Rolling bearing plays an important role in rotary machines and it is also one of the main sources for the breakdown of mechanical equipment. Rolling bearings fall out of work are often for various reasons, such as unexpected heavy loads, lack of lubrication and ineffective sealing [1]. Statistics suggest that almost thirty percent of the failures in rotating machinery are caused by the damaged bearings. Therefore, it is vital to detect bearing fault and decrease possible financial and production loss [2]. Over the past several decades, many researchers have focused their work on the

bearing fault detection and diagnosis. And these methods can be divided into three categories depending on the procedure of their diagnosis, i.e., data based, model based and signal based [3,4]. Nevertheless, signal processing is always an important part in the three categories. And these signal processing techniques can be classified into time domain, frequency domain and time-frequency domain [5].

In bearing fault diagnosis, there are several types of faults frequently happening, namely outer race faults, inner race faults and rolling element faults [6,7,8]. The main goal of fault diagnosis is to determine whether the bearing's state is normal. Assuming that the state is

abnormal, what's more, we should also make sure which faulty category it is. And the popular techniques for signal analysis mainly include three types mentioned in the above paragraph. Chen and Wang in [9,10] combined the time series analysis algorithm with neural network to complete the detection and fault diagnosis. In [11], FFT of IMFs from Hilbert-Huang Transform process has been merged to utilize the efficiency of Hilbert Transform in frequency domain. For the frequency-domain analysis, we can examine the frequencies typical for the fault to identify the occurrence of fault. Besides, it can even identify the faulty category, like failure in outer race or in the inner race [1]. In [12], vibration signals are decomposed into a number of product functions through local mean decomposition algorithm and multi-scale entropy of each product function is calculated as feature vectors. And then, these feature vectors act as the input of fault classifier so as to complete faulty classification. However, all of these methods mainly make use of the vibration signal processing techniques in 1-dimensional domain.

However, researchers tend to complete faulty classification through image processing methods in two-dimension domain. Especially in computer vision systems, various algorithms turn out to be effective[13,14,15]. They try to transform the vibration signals into images and image processing methods are employed to obtain the bearing's state. Shahriar and Chong in [3] proposed a method for fault diagnosis utilizing local binary pattern-based texture analysis. They utilized the LBP algorithm to extract texture features from images and extracted features are then used by multi-class support vector machine to identify the faults of induction motors. In [16], Do and Chong proposed a method for vibration signal-based fault detection and diagnosis system applying for induction motors. The method included fault detection process and fault diagnosis process. In fact, it transformed the vibration signals into images and feature descriptors are extracted from the images based SIFT algorithm. The 128-dimensional keypoint descriptors produced by the SIFT algorithm were then used to achieve the classification of inductor faults. The method was claimed to be robustness for the fact that noises in the vibration signals were regarded as illumination variation when transformed into images. And SIFT algorithm is proved to maintain a degree of stability for

image rotation, scale variation and illumination changes [3,17]. However, it indeed exist some limitations of applying this method for the fault diagnosis of rolling bearings. One of the limitations is the high computation cost for the processing of 128-dimensional descriptors. And another one is that the number of feature descriptors for each image is uncertain, sometimes the number may even be too small to classify the type of faults.

In this paper, we proposed an improved approach based on the method mentioned above. The proposed detection and fault diagnosis system provides an improvement over existing methods at various aspects. During preprocessing, normalized vibration signals are transformed into images. And images are enhanced by using mean filter before they are processed with image processing methods. During feature extraction, we make use of Speeded Up Robust Features (SURF) instead of SIFT algorithm. SIFT and SURF algorithms employ slightly different ways of detecting features [18]. And in [19], the detector and descriptor of SURF is proved to be faster, at the same time, the detector is also more repeatable and the descriptor is more distinctive. Compared to SIFT algorithm, SURF is more sensitive to illumination changes and image blur [18]. Images transformed from vibration signals are mainly affected by illumination changes and image blur. Namely, SURF outperforms SIFT algorithm in computation cost and classification accuracy. Considering the advantages mentioned above, in this paper, feature descriptors are extracted from the images enhanced by the mean filter based on SURF algorithm. And through the mean-shift clustering algorithm, a texture dictionary related to each faulty category is formed. After that, feature descriptors extracted from testing images are compared to the texture dictionary, and the descriptor vectors are matched between different images in texture dictionary. The matching is based on a Euclidean distance between the vectors. The performance of the proposed method has been evaluated for 4 different bearing operating conditions under a laboratory environment. Additionally, a comparative experiment with the existing method has done. The results show that our proposed approach is more suitable for bearing fault diagnosis.

Nowadays, various image processed algorithms have occurred and they are proved to be effective in image classification. The introduction of image

processed algorithm in bearing fault diagnosis turns out to be new, but useful. It seems to show us a new way for bearing fault diagnosis.

The rest of the paper is organized as follows. In section 2, the theory of SURF algorithm is briefly introduced. The fault diagnosis system based on SURF algorithm is proposed in Section 3. Section 4 presents the experimental setup of data acquisition. The results of the proposed fault diagnosis system are given in Section 5 and compared with the existing SIFT method. And the conclusion is presented in the last section.

## 2 Speeded Up Robust Features (SURF)

SURF is developed from the SIFT algorithm, and it is a novel detector-descriptor scheme. SURF (Speeded Up Robust Features) is a robust local feature detector, firstly presented by Herbert Bay et al. in 2006. And it is widely used in computer vision areas. SURF algorithm shares the same matching approach with SIFT but with a few variations [20]. Firstly, the SURF detector is based on Hessian matrix and it uses the integral images to reduce the computational time [19,20,21]. Secondly, the descriptor vectors in SURF are only 64-dimensional compared to 128 dimensions in SIFT. This can also reduce the time for computation and matching. And features based on SURF are proved to be very distinctive and stable. A briefly description about the SURF algorithm is discussed below.

### 2.1 SURF detector

The SURF detector is mainly used to detect the interest point and we therefor call it interest point detector. Different from the image pyramids building in SIFT, we use the approximation image based on the determinant of Hessian matrix in SURF. The SURF detector is based on the Hessian matrix for its excellent performance in computation time and accuracy [19]. Given a point  $D = (x, y)$  in an image, the Hessian matrix  $H(D, \sigma)$  in point  $D$  at scale  $\sigma$  is as follows [11]:

$$H(D, \sigma) = \begin{bmatrix} L_{xx}(D, \sigma) & L_{yx}(D, \sigma) \\ L_{xy}(D, \sigma) & L_{yy}(D, \sigma) \end{bmatrix} \quad (1)$$

where  $L_{xx}(D, \sigma)$  is the convolution of the Gaussian second order derivative  $\partial^2 g(x)/\partial x^2$  with the image

in point  $D$ , the similar to the obtaining of  $L_{xy}(D, \sigma)$  and  $L_{yy}(D, \sigma)$ . The approximations of Gaussian second order derivative for  $9 \times 9$  filters are denoted by  $D_{xx}$ ,  $D_{xy}$  and  $D_{yy}$ , where  $D_{xx}$  refers to the approximation for the second order Gaussian partial derivative in  $x$  direction, the same with  $D_{yy}$  and  $D_{xy}$ . The determinant of the Hessian is computed as follows:

$$\det(H_{approx}) = D_{xx}D_{yy} - (\omega D_{xy})^2 \quad (2)$$

where  $\omega$  is discussed in [19] and it optimized to be 0.9 for the purpose of balancing the expression for the Hessian's determinant.

Due to the use of box filters and integral images, we have no need to continuously apply the same filter to the output of the previously filtered layer just like we do in SIFT. Instead, we can just apply box filters of any size at exactly the same speed directly on the original image [19]. The integral image  $I_{\Sigma}(D)$  represents the sum of all pixels in the input image  $I$  within a rectangular region formed by the point  $D$ , and the integral image in point  $D = (x, y)$  can be defined as follows:

$$I_{\Sigma}(D) = \sum_{i=0}^x \sum_{j=0}^y I(i, j) \quad (3)$$

Interest points are located in the image and over scales by applying a non-maximum suppression in a  $3 \times 3 \times 3$  neighborhood. The maxima of the Hessian's determinant are then interpolated in scale and image space. For the difference in scale between each octave in the image pyramid, interpolation in scale space is especially important.

### 2.2 SURF descriptor

In order to obtain the descriptor, we may just need two steps. Firstly, we need to select a dominant orientation for each interest point. Within the circular neighborhood of interest point (i.e., a circle of  $6s$  radius,  $s$  is the scale of the point), a sliding orientation window of size  $\pi/3$  is used to calculate the Haar wavelet responses in both horizontal and vertical directions. The calculated responses then yield a local orientation vector. The orientation of the interest point is defined by the orientation of the longest vector over all windows. Fig.1 shows the procedure of orientation assignment.

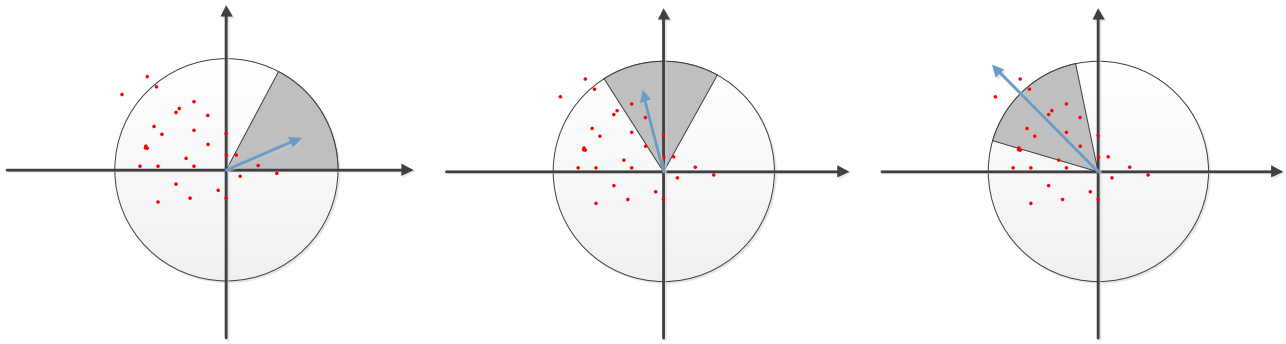


Fig.1. Orientation assignment

The next step, we construct a square region around the interest point, and the square region shares the same orientation with the dominant direction detected earlier. We divide the region into  $4 \times 4$  square sub-regions [22,23,24]. For each sub-region, the wavelet responses are computed at  $5 \times 5$  regularly spaced sample points. And in each sub-region, we calculate the sum of Harr wavelet responses in the horizontal and vertical directions ( $d_x$  and  $d_y$ , where the horizontal and vertical direction is relative to the dominant orientation mentioned in the first step). We also calculate the sum of the absolute value of the

responses,  $|d_x|$  and  $|d_y|$  (See in Fig.2). And the feature of each sub-region can be described as follows:

$$v = (\sum d_x, \sum d_y, \sum |d_x|, \sum |d_y|) \quad (4)$$

Hence, for the whole  $4 \times 4$  regions, the length of each feature descriptor vector is 64. Compared to the 128-dimensional descriptors in SIFT, our obtained descriptor vectors decrease time cost in the matching stage to some extent.

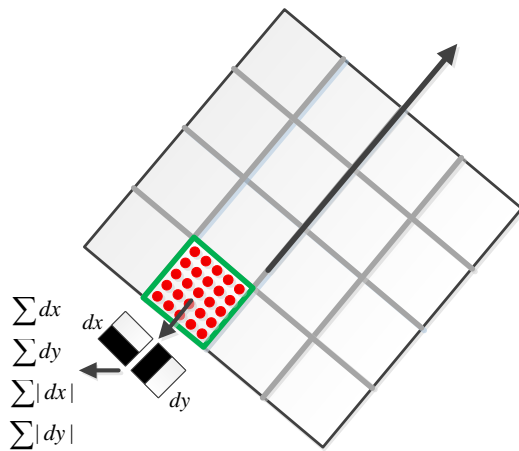


Fig.2. The procedure of building the descriptor

### 3 Fault diagnosis method based on Surf

Vibration signals are first normalized and then transformed to gray-scale images. Images of different faulty categories have different texture features. We extract feature vectors from images of all faulty categories and form a texture dictionary through the clustering algorithm based on the extracted feature vectors. Finally, feature vectors obtained from testing signals are compared to the texture dictionary to compete the fault classification. The procedure of our proposed method is shown in Fig.3.

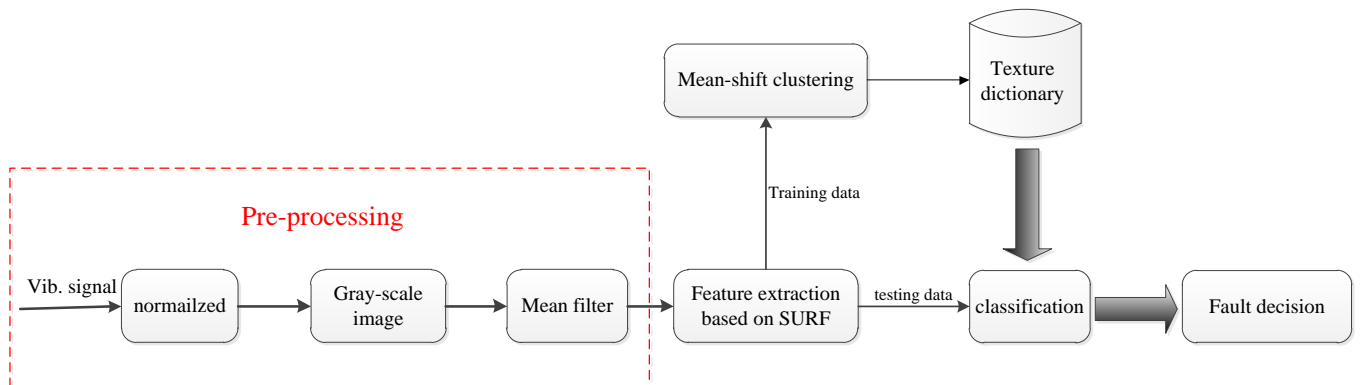


Fig.3. Procedure of the proposed fault diagnosis system

### 3.1 Pre-processing

During pre-processing, the amplitude of each vibration signal is normalized ranging 0 from 1 in type of double. After that, normalized signals are converted into gray-scale images and the amplitude turns into the pixel intensity of an image. The size of the image is dependent on the length of a vibration signal. In order

to make sure that the signal contains enough faulty information, the length is expected to be long enough. However, the longer the signal is, the more computation cost we need. Given a vibration signal of length  $L$ , the size of the transformed image is supposed to be  $M \times N$ . The conversion scheme is shown in Fig.4.

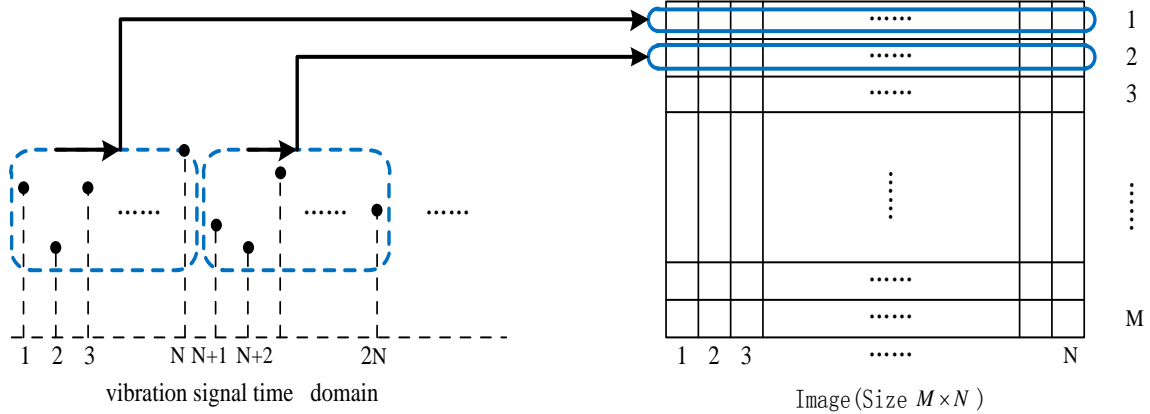


Fig.4. Scheme of vibration signal to image

After the conversion, we try to enhance the image by dealing it with a mean filter. A vibration signal and its gray-scale image enhanced by a mean filter are

shown in Fig.5. The length of the signal is 16348, and the image is considered to be  $128 \times 128$ .

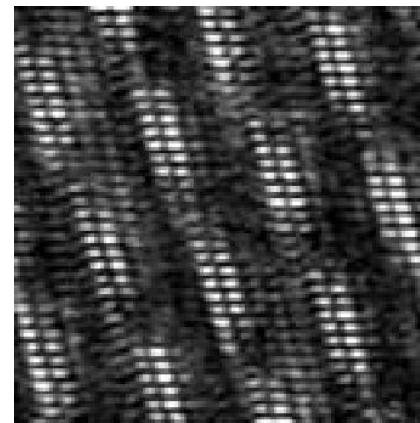
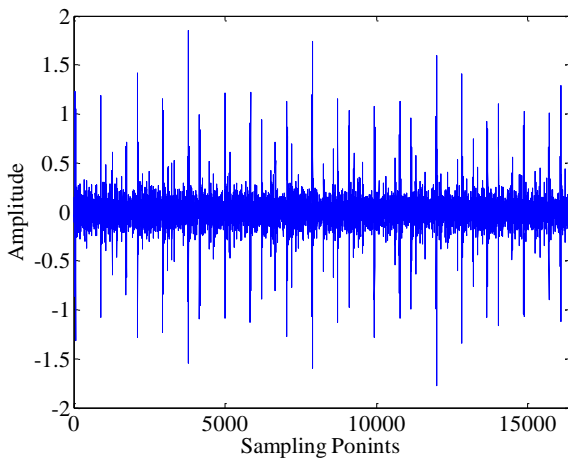


Fig.5. Vibration signal and its gray-scale image enhanced by a mean filter

### 3.2 Texture dictionary

Images transformed from vibration signals usually have rich texture features, and texture feature varies in different faulty categories. SURF is a computer vision algorithm and it can make full use of the texture features of an image. The existence of fault related frequencies makes the special texture features, and noises are regarded as changes in illumination. SURF

algorithm is proved to be more sensitive to illumination changes and image blur in [18]. What's more, the 64-dimensional descriptor vectors in SURF can decrease the computation time when compared to SIFT algorithm. Hence, feature extraction based on SURF algorithm can be reliable.

In the proposed method, SURF algorithm is applied to detect the interest points and generate the

64-dimensional feature vectors. These feature vectors can fully represent the local feature of the image. In order to include all of the faulty categories, we conduct four vibration signals of different categories, i.e., inner race fault, outer race fault, rolling element fault and normal condition. Feature vectors extracted from images of different faulty categories are clustered to form a texture dictionary through the mean-shift clustering algorithm. Through the clustering algorithm, texture dictionary has fewer vectors, but it turns to be more representable and reliable for all kinds of faulty categories. The following work is to classify the testing image into its corresponding faulty category.

### 3.3 Fault classification

As mentioned above, texture dictionary is generated by analyzing the fault signals of all kinds. Texture dictionary and feature vectors extracted from testing images are used to achieve the goal of fault classification. Firstly, we choose a testing vibration signal and transform it into a gray-scale image. Through the mean filter, the image is enhanced. After that, feature vectors are extracted from the enhanced image based on SURF algorithm. Finally, feature vectors extracted from testing image are compared to

the texture dictionary and testing signal can be classified to its corresponding faulty category.

During the matching process, the Euclidean distance between each extracted feature vector and the centroid feature vectors in texture dictionary are calculated. The centroid feature vector generating the minimal distance is called to be “matched” vector and the category containing the highest number of “matched” vector is classified to be the fault category of the testing signal.

## 4 Method Verification

### 4.1 Experimental Setup

An experimental rig was constructed to obtain the vibration signals. As shown in Fig.6, the test rig consists of a motor, two bearing pedestals, a base and a coupling. The bearings are installed in a motor driven mechanical system. Two acceleration sensors located in the vertical directions are used to acquire the vibration signals under four types of faults (inner race fault, outer race fault, rolling element fault and normal condition). The rotational speed of the motor is set to be 900r/min, 1200r/min, 1500r/min and the sampling frequency is 10 kHz.

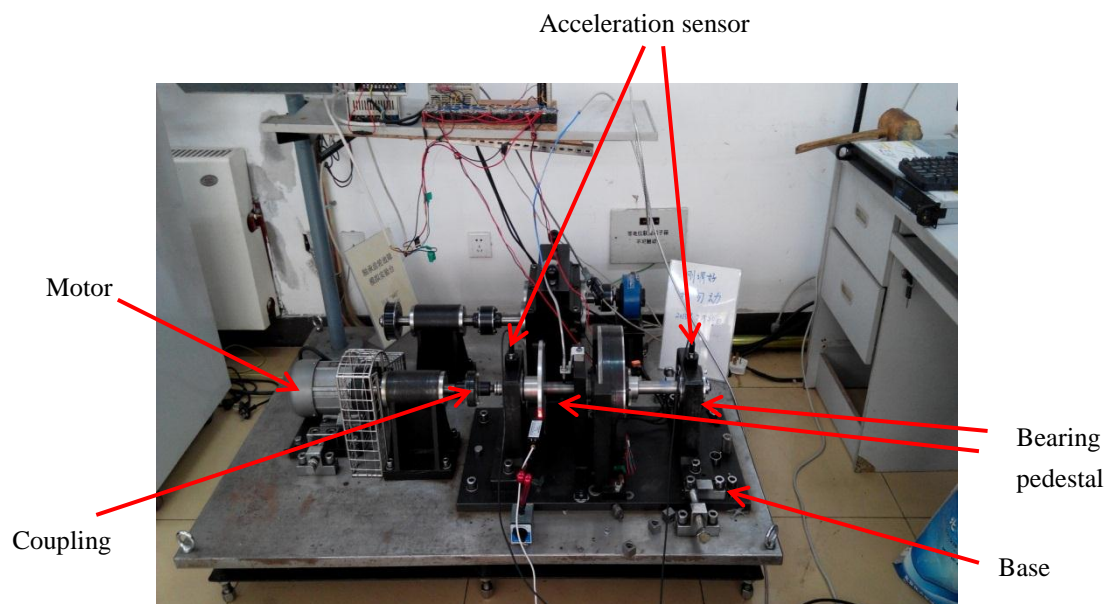


Fig.6. Experimental rig

### 4.2 Experiment analysis

Each signal sample is acquired with 16348 points (about 40 circles of vibration signal for the 1500r/min speed) and its image size is  $128 \times 128$ . Six signal

samples are obtained for each category in three different rotational speeds. We take one sample signal from each fault category as the training dataset and the others act as testing dataset. Namely, we have four

training signals and twenty testing signals in each rotational speed. Totally, we get 12 training signals and 60 testing signals. Training signals are used to form the texture dictionary and testing signals are used to evaluate the performance of the proposed method. The four training vibration signals under the 1500r/min speed and their images enhanced by the mean filter are shown in Fig.7.

In order to exhibit the superiority of the proposed diagnosis system, an experiment is conducted on testing dataset to evaluate its performance. An enhanced testing image from the testing dataset is

shown in Fig.8. We extract feature vectors from the testing image and compare them to the feature vectors in the texture dictionary. The number of the “matched vector” is drawn in histogram, as shown in Fig.9. Through the histogram, we can see that there are 352 feature vectors and 232 “matched” vectors for Inner race fault, 0 for outer race fault, 24 for rolling element fault and 96 for normal condition. The highest number belongs to the inner race fault category, so we determine the testing signal to be inner race fault category.

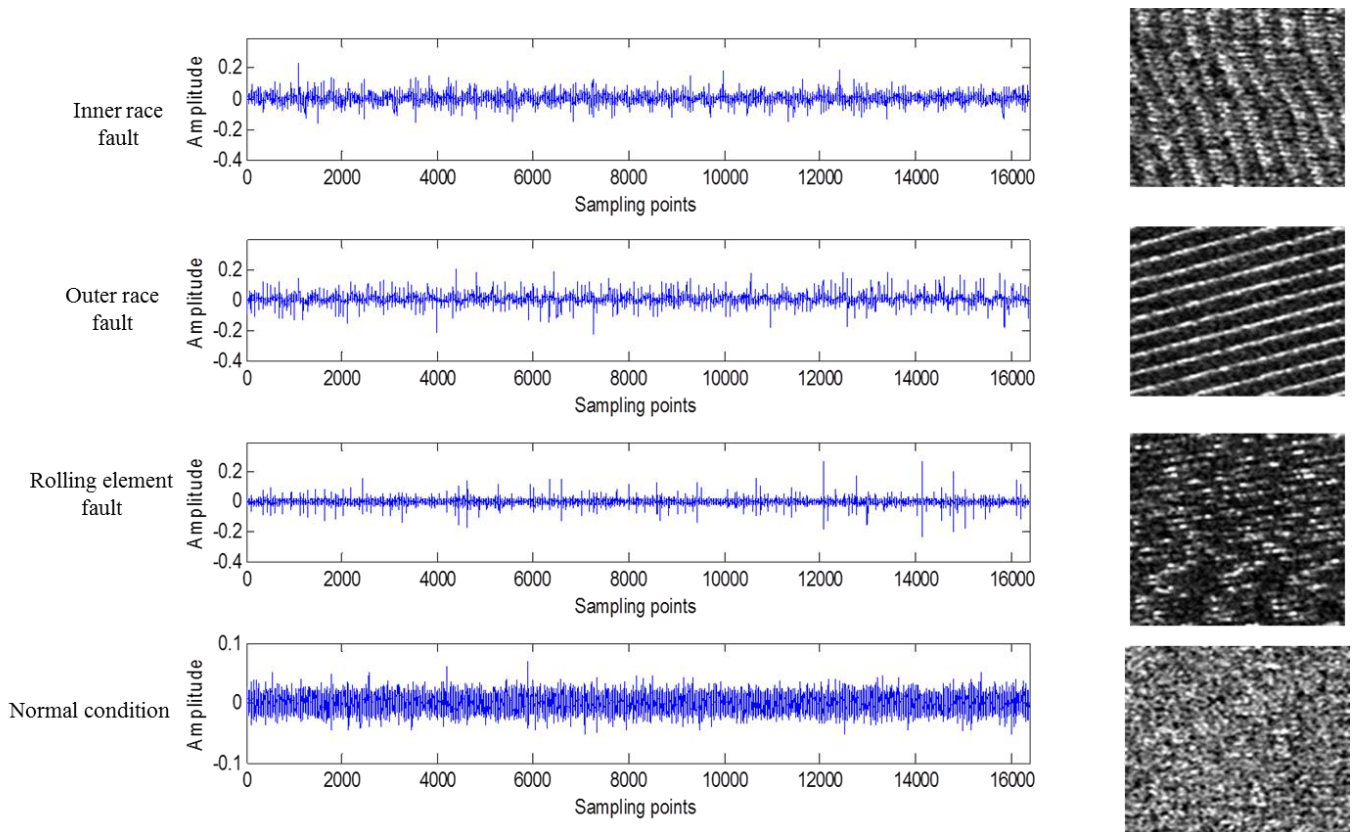


Fig.7. Vibration signal in the training dataset and their enhanced images

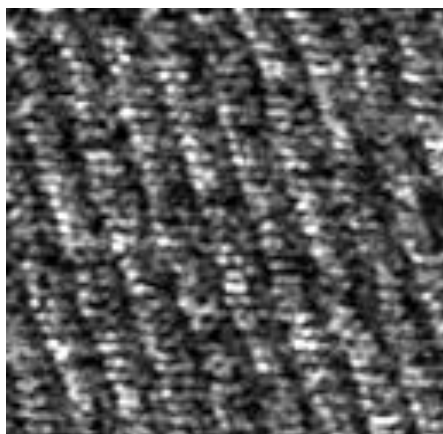


Fig.8. Enhanced testing image

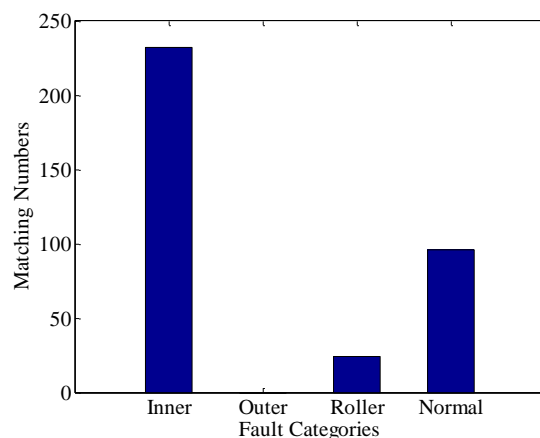


Fig.9. Histogram of matched numbers

To illustrate the number of “matched” vector in each testing signal, four testing signals of different types are investigated. Table 1 shows the percentage of “matched” number for each category. The highest percentage number indicates the corresponding faulty categories that the vibration signal belongs to.

As mentioned above, 60 testing signals are obtained under our experimental condition. Table 2 shows the classification accuracy of the whole testing signals. The experiment results indicate that each fault category can get a high classification accuracy and the proposed system is effective in our bearing fault diagnosis. Additional, vibration signals obtained from the Case Western Reserve University Bearing Data

Center are also applied in the proposed system. The proposed fault diagnosis system still demonstrates its excellent fault classification performance.

To demonstrate the improved accuracy of the proposed approach for identifying the faults of rolling bearing, the proposed system is compared with the method used in [16]. In this comparison, each vibration signal shares 16348 sampling points and its image size is  $128 \times 128$ . The vibration signals are from the bearing data center [25]. The rotational speed of the motor is 1750r/min and the sampling frequency is 12 kHz. The comparison of the classification accuracy between the two proposed methods is shown in Table 3.

Table 1 Percentage of “matched” number for each category

Signal (Belonged category)	Percentage of “matched” number for each faulty category (%)			
	Inner race fault	Outer race fault	Rolling element fault	Normal condition
Inner race fault	68.47	0	7.67	23.86
Outer race fault	0	98.73	1.27	0
Rolling element fault	12.57	1.6	71.93	13.9
Normal condition	13.95	0	2.03	84.01

Table 2 Classification accuracy for different faulty categories under three different rotational speeds

Rotational speed of the motor	Classification accuracy for different faulty categories (%)			
	Inner race fault	Outer race fault	Rolling element fault	Normal condition
900r/min	83.3	100	83.3	100
1200r/min	100	100	83.3	100
1500r/min	100	100	100	100

Table 3 Comparison of proposed system and the approach proposed in [16]

	Classification accuracy for different faulty categories (%)			
	Inner race fault	Outer race fault	Rolling element fault	Normal condition
Proposed system	100	100	100	100
SIFT-based approach	100	100	83.3	50

On the grounds of the above experimental results, the proposed method based on SURF algorithm earns higher classification accuracies and decreases computation time theoretically. Therefore, the proposed method is supposed to be more suitable for bearing fault diagnosis.

## 5 Conclusions

In this paper an effort has been made to develop a robust fault diagnosis system for rolling bearing. The proposed approach translates the input vibration signals into gray-scale images for the fault classification of the rolling bearing. SURF-based algorithm is introduced, for the sake of extracting texture features from the images. The proposed method



applies to rolling bearings and effectively classifies each vibration signal to its corresponding fault category. Therefore, it is a powerful method for fault diagnosis of rolling bearings. In addition, to prove the improved classification performance of the proposed system, the proposed approach is compared with the SIFT-based method. The experimental results indicate that the proposed approach offers higher classification accuracies.

Resuming, in this paper, the propose fault diagnosis system seems to show a new way for bearing fault diagnosis. Different from the classical signal processed methods in bearing fault diagnosis, feature extraction algorithms based on gray-scale image are introduced. The proposed fault diagnosis system translates the time-series signals into visual images. Thus, noises in the vibration signal are turned into different gray levels. These image features are then used to reach the goal of fault classification. However, this method is proved to be more useful and suitable for rolling bearing fault diagnosis. Future research will be focus on the identification of multiple bearing fault diagnosis.

## Acknowledgements

This project is supported by National Natural Science Foundation of China (Grant No. 51375037) and Program for New Century Excellent Talents in University (NCET-12-0759).

### Reference:

- [1] Jacek Dybala, and Radoslaw Zimroz, Rolling bearing diagnosing method based on Empirical Mode Decomposition of machine vibration signal, *Applied Acoustics*, 77:195-203, 2014.
- [2] Li Jiang, Jiangping Xuan, and Tielin Shi, Feature extraction based on semi-supervised kernel Marginal Fisher analysis and its application in bearing fault diagnosis, *Mechanical Systems and Signal Processing*, 41: 113-126, 2013.
- [3] Md Rifat Shahriar, Tanveer Ahsan, and UiPil Chong. Fault diagnosis of induction motors utilizing local binary pattern-based texture analysis, *EURASIP Journal on Image and Video Processing*, 29, 2013.
- [4] Peng Wang, Hongfang Yuan, Huaqing Wang, Xi Cao, and Xuewei Wang, Rolling Element Bearing Fault Diagnosis Based on Symptom Parameter Wave of Acoustic Emission Signal, *Advanced Science Letters*,13(1): 667-670, 2012.
- [5] Hongfang Yuan, Fangming Li, and Huaqing Wang, Using Evaluation and Leading Mechanism To Optimize Fault Diagnosis Based on Ant Algorithm, *Energy Proscenia*, 1(6): 112-116, 2012.
- [6] Zuoyi Dong, Huaqing Wang, Wang Shuming, Wei Hou and Qingliang Zhao, Intelligence diagnosis method based on particle swarm optimized neural network for roller bearings. *WSEAS Transactions on Systems*, 12:667-677, 2013.
- [7] Bo Li, Mo-Yuen Chow, and James C. Huang, Neural-Network-Based Motor Rolling Bearing Fault Diagnosis, *IEEE Transactions on industrial electronics*, 47: 1060-1069, 2000.
- [8] Huaqing Wang, Wei Hou, Gang Tang, Hongfang Yuan, Qingliang Zhao and Xi Cao, Fault Detection Enhancement in Rolling Element Bearings via Peak-Based Multiscale Decomposition and Envelope Demodulation, *Mathematical Problems in Engineering*, 2014.
- [9] Gang Chen, Yang Liu, Wen-an Zhou and Jun-de Song, Research on Intelligent fault diagnosis based on time series analysis algorithm, *The Journal of China universities of posts and telecommunications*, 68-74, 2008.
- [10] Chun-Chieh Wang, Yuan Kang, Ping-Chen Shen, Yeon-Pun Chang, and Yu-Liang Chung, Application of fault diagnosis in rotating machinery by using time series analysis with neural network, *Expert Systems with Applications*, 37: 1696-1702, 2010.
- [11] V. K. Rai, and A. R. Mohanty, Bearing fault diagnosis using FFT of intrinsic mode functions in Hilbert-Huang transform, *Mechanical System and Signal Processing*, 21: 2607-2615, 2007.
- [12] Huanhuan Liu, and Minghong Han, A fault diagnosis method based on local mean decomposition and multi-scale entropy for rolling bearings, *Mechanism and Machine Theory*, 75 : 67-78, 2014.
- [13] M. Papoutsidakis, D. Piromalis, F. Neri, and M. Camilleri, Intelligent Algorithms Based on Data Processing for Modular Robotic Vehicles Control, *WESEAS Transactions on Systems*,13,WSEAS

- Press,242-251, 2014.
- [14] Camilleri M., Neri F., and Papoutsidakis M. An Algorithmic Approach to Parameter Selection in Machine Learning using Meta-Optimization Techniques, *WSEAS Transactions on Systems*, 13, WSEAS Press, 202-213, 2014.
- [15] S. Staines A., and Neri F., A Matrix Transition Oriented Net for Modeling Distributed Complex Computer and Communication Systems, *WSEAS Transactions on Systems*, 13, WSEAS Press, 12-22, 2014.
- [16] Van Tuan Do, and UoPil Chong, Signal Model-based Fault Detection and Diagnosis for Induction Motors Using Features of Vibration Signal in Two-dimension Domain, *Journal of Mechanical Engineering*, 57: 655-666, 2011.
- [17] David G. Lowe, Distinctive Image Features from Scale-Invariant Keypoints, *International Journal of Computer Vision* Vol.60, No.2, 91-110, 2004.
- [18] Luo Juan, and Oubong Gwun, A comparison of SIFT, PCA-SIFT and SURF, *International Journal of Image Processing* Vol.3, No.4, 143-152, 2009.
- [19] Herbert Bay, Andreas Ess, Tinne Tuytelaars and Luc Van Gool, Speeded-Up Robust Features(SURF), *Computer Vision and Image Understanding*, 110: 346-359, 2008.
- [20] Hunny Mehrotra, Pankaj K. Sa, and Banshidhar Majhi, Fast segmentation and adaptive SURF descriptor for iris recognition, *Mathematical and Computer Modeling*, 58: 132-146, 2013.
- [21] Aldo Cumani, and Antonio Guiducci, Fast Point Features for Accurate Visual Odometry, *12<sup>th</sup> WSEAS International Conference on Systems*, 186-191, 2008.
- [22] C. Valgren, and A. Lilienthal, SIFT, SURF and Seasons: long-term outdoor localization using local features, *in: 3rd European Conference on Mobile Robotics*, 2007.
- [23] A.C. Murillo, J.J. Guerrero, and C. Sagues, SURF features for efficient robot localization with omnidirectional images, *IEEE International Conference on Robotics and Automation*, 3901–3907, 2007.
- [24] H. Bay, T. Tuytelaars, and L. Van Gool, SURF: Speeded Up Robust Features. *In Ninth European Conference on Computer Vision*, 2006
- [25] K. A. Loparo, Bearings Vibration Data Set, Case Western Reserve University, (<http://csegroups.case.edu/bearingdatacenter/pages/download-data-file>)